Available online at www.sciencedirect.com
ScienceDirect
Trans. Nonferrous Met. Soc. China 21(2011) s1−s6
Transactions of Nonferrous Metals Society of China
www.tnmsc.cn

Microstructure and properties of alumina-silicon carbide nanocomposites fabricated by pressureless sintering and post hot-isostatic pressing

Young-Keun JEONG[1], Koichi NIIHARA[2]

1. National Core Research Center for Hybrid Materials Solution, Pusan National University, Busan 609-735, Korea;
2. Nagaoka University of Technology, Niigata 940-2188, Japan

Received 21 April 2010; accepted 10 September 2010

Abstract: Al_2O_3/5%SiC nanocomposites were fabricated by pressureless sintering using MgO as a sintering aid and then post hot-isostatic pressed (HIP), which can subsequently break through the disadvantage of hot-pressing process. The MgO additive was able to promote the densification of the composites, but could not induce the grain growth of Al_2O_3 matrix due to the grain growth inhibition by nano-sized SiC particles. After HIP treatment, Al_2O_3/SiC nanocomposites achieved full densification and homogeneous distribution of nano-sized SiC particles. Moreover, the fracture morphology of HIP treated specimens was identical with that of the hot-pressed Al_2O_3/SiC nanocomposites showing complete transgranular fracture. Consequently, high fracture strength of 1 GPa was achieved for the Al_2O_3/5%SiC nanocomposites by pressureless sintering and post HIP process.
Key words: nanocomposite; pressureless sintering; fracture strength

1 Introduction

Ceramic nanocomposites represent a new class of materials with significantly improved mechanical properties, even at high temperatures, compared with monolithic ceramics. One notable system is Al_2O_3/SiC nanocomposite because of distinguishably improved mechanical properties. It has been reported by NIIHARA et al[1−4] that a dispersion of 5% SiC nano-particles into Al_2O_3 could remarkably increase the room temperature strength from 350 MPa to higher than 1 000 MPa. In addition, the fracture toughness and creep resistance were also improved by in-grain toughening associated with intragranular SiC particulates[5] and grain boundary strengthened by intergranular SiC dispersions[6−7], respectively.

Generally, these nanocomposites are fabricated with high densities by hot-pressing process because of the difficulty in densifying the composites. However, this process can only manufacture ceramic particles with simple geometrical shapes, and would be expensive and unsuitable for mass production. For many potential applications of these materials, pressureless sintering process would be preferable if full density is achieved.

There were some studies on fabricating the Al_2O_3/SiC nanocomposites by pressureless sintering process[8−12]. BORSA et al[8] fabricated Al_2O_3/5%SiC (mass fraction) nanocomposite by a pressureless sintering route to a maximum relative density of about 95%. ZHAO et al[9] sintered Al_2O_3/5% SiC (volume fraction) nanocomposite to a relative density of 98.3% by the same route. ANYA and ROBERTS[10] also reported that Al_2O_3/SiC nanocomposites with high relative density (≥99.6%) and with up to 15% SiC (volume fraction), were fabricated by pressureless sintering. However, improved strength of pressureless sintered Al_2O_3/SiC nanocomposites has not been reported.

The objective of this work is to fabricate Al_2O_3/SiC nanocomposites with high fracture strength by pressureless sintering and hot-isostatic pressing (HIP) technique which can subsequently break through the disadvantage of hot-pressing process. It is well known that a small addition of MgO is favorable to inhibit the discontinuous grain growth and to promote the sintering of monolithic Al_2O_3, which leads to full density[13−15]. Accordingly, MgO was selected as a sintering aid, and the effects of MgO addition on the microstructures and mechanical properties of Al_2O_3/SiC composites were investigated.

Foundation item: Project supported by Pusan National University Research Grant; Project(2010-0008-276) supported by National Core Research Center Program through the National Research Foundation of Korea funded by the Ministry of Education, Science and Technology
Corresponding author: Young-Keun JEONG; Tel: +82-51-5102483; E-mail: nano@pusan.ac.kr

The pressureless sintering and post HIP process employed in the present work consist of two steps: 1) a normal sintering procedure to eliminate open pores in specimens, and 2) a second sintering under a high isostatic gas pressure. Finally, this study focused on conventional processing techniques as a relatively simple and cost-effective method adequate for mass production.

2 Experimental

2.1 Materials

The α-Al_2O_3 powder used in this study (TM-DAR, Taimei Chemicals Co., Nagano, Japan) had a purity of 99.99%, mean particle size of 0.21 μm and specific surface area of 14.7 m^2/g (all quoted by manufacturer). β-SiC powder (Ibiden Co., Gifu, Japan) had a mean particle size of 0.27 μm (average grain size of 70 nm by TEM) and specific surface area of 23.5 m^2/g. High pure MgO (Ube Co., Yamaguchi, Japan) with a mean particle size of 0.1 μm was used as a sintering additive. The starting powders were weighed with 5%SiC (volume fraction). In order to investigate the effects of MgO, different amounts of MgO (0.05%, 0.1% and 0.3%) were added to Al_2O_3/SiC powders. The combined powders were ball-milled in ethanol for 24 h using high-purity Al_2O_3 balls with diameter of 5 mm in a polyethylene pot. Then, soft agglomerates of the dried powders were crushed by dry ball-milling for 24 h using Al_2O_3 balls with diameter of 10 mm.

The mixed powders and as-received Al_2O_3 powder were uniaxially pressed at 30 MPa into bars with dimensions of 5.5 mm×6.4 mm×53 mm, and isostatically pressed at 200 MPa. The powder compacts, which were laid on graphite foil without any powder bed in a covered graphite crucible, were sintered in flowing argon at various temperatures for 2 h. The subsequent HIP treatment was carried out at 1 600 °C for 1 h under argon atmosphere at 150 MPa. The specimens before and after HIP treatment were ground with a diamond wheel for mechanical testing. The tensile surfaces of the bars for three-point bending test were polished using diamond paste to 1 μm finish and the edges on tensile surface were beveled at 45°. The dimensions of the machined specimens were approximately 3 mm×4 mm×42 mm.

2.2 Characterization

The relative densities of the specimens before and after HIP treatment were measured by using water-immersion method, and the open porosity (P_o) was determined from the relation

$$P_o=(m_2-m_1)/(m_2-m_3)\times100 \quad (1)$$

where m_1, m_2, and m_3 are the mass of the dry specimen, the mass of the same specimen saturated with boiling water and the suspended mass of the saturated specimen in water, respectively. The fracture strength was measured by three-point bending test with a span of 30 mm at a cross-head speed of 0.5 mm/min. For microstructural observation by scanning electron microscopy (SEM), the polished specimens were thermally etched at 1 450 °C for 15 min in flowing argon. The grain sizes were deduced from the SEM micrographs of the etched surfaces by using a computer program for image analysis (NIH image). This software measures the area of each grain, and converts the area into an equivalent circle to obtain its equivalent diameter. At least 400 grains were measured for each sample. The distribution of SiC particles was identified by transmission electron microscopy (TEM). Specimens for TEM were thinned to electron transparency by mechanical grinding followed by ion beam milling.

3 Results and discussion

3.1 Densification behavior

Fig.1 shows the densification behaviors of pressurelessly sintered Al_2O_3/5%SiC (volume fraction) composites with different MgO contents. The sintered density of Al_2O_3/SiC composites was significantly improved by the addition of MgO sintering aid, regardless of sintering temperature. As the amount of MgO increased to 0.1% (mass fraction), the sintered density increased remarkably. When the amount of MgO increased from 0.1% to 0.3% (mass fraction), density improvement was not observed any more.

Some experimental studies clearly demonstrate that monolithic Al_2O_3 can be sintered to a maximum density at a critical MgO content. PEELEN[14] sintered Al_2O_3 specimens containing MgO up to 0.3% and reported that a maximum density near to theoretical density was found at 0.03% MgO. BAE and BAIK[16] reported that a maximum density of pure Al_2O_3 was also achieved at

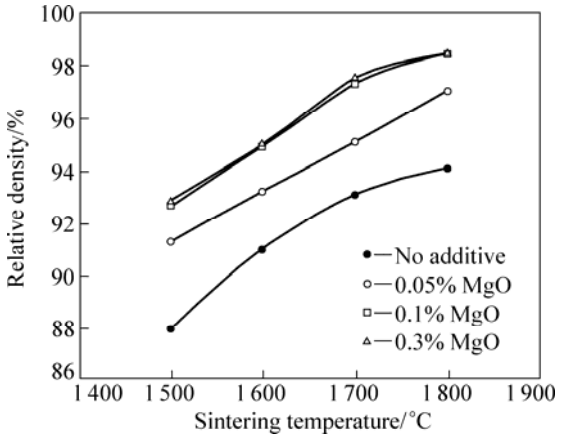

Fig.1 Relative density as function of sintering temperature for Al_2O_3/5%SiC composites with different MgO contents

0.03%MgO addition, but this critical MgO content increased with increasing impurity content in Al_2O_3. In this study, a small amount of impurities may be introduced into Al_2O_3/SiC powder mixtures from the starting powders, mainly SiO_2 in SiC powder and ball wear during ball-milling process[17]. Accordingly, the increase of MgO content required to achieve a maximum density may be associated with these impurities.

In sintered ceramic materials, open pores are generally eliminated when the bulk density reaches 93%−95%[18−20], which is essential to the pressureless sintering and post HIP process. In Al_2O_3/SiC composite systems, in contrast to monolithic Al_2O_3, however, the open pores disappeared dramatically at the bulk density of about 90%, as shown in Fig.2. Therefore, the full densification could be achieved by HIPping Al_2O_3/SiC specimens with sintered bulk density higher than 91%, as shown in Fig.3.

Some commercial Al_2O_3 powders used in previous

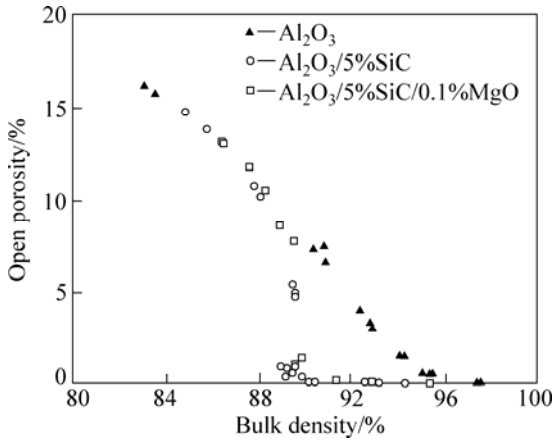

Fig.2 Open porosity as function of bulk density for monolithic Al_2O_3 and Al_2O_3/5%SiC composites without and with 0.1% MgO

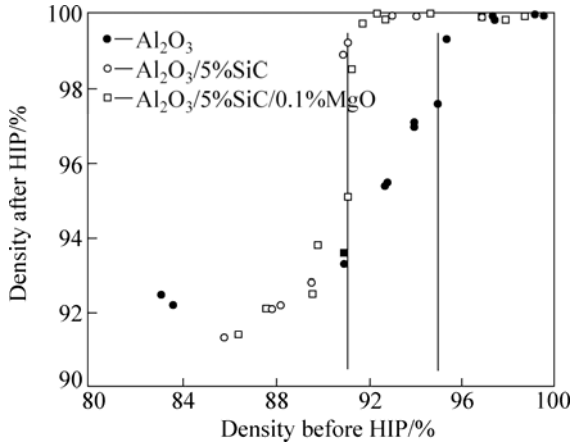

Fig.3 Variations of HIP density with sintered density for monolithic Al_2O_3 and Al_2O_3/5%SiC composites without and with 0.1% MgO

experiments had a large amount of background impurities to form a liquid phase during sintering[21−24]. HANSEN and PHILLIPS[23] found that nearly all grain boundaries of a commercial 99.8% Al_2O_3 were wet by an amorphous film containing SiO_2 and CaO in addition to Al_2O_3. HARMER[24] found that a thin glassy film at grain boundaries was formed even in high pure 99.98% Al_2O_3. Therefore, the sudden change of open porosity observed in this work may be caused by a small amount of liquid phase which was originated from impurities as mentioned above. This liquid phase may be a metastable aluminosilicate glass phase that can be formed during the reaction of Al_2O_3 with the surface silica layer on SiC powder. The location of liquid phase in the microstructure depends on the local wetting conditions for grain boundaries and on the volume fraction of liquid phase[25]. For small amounts of liquid, however, the liquid prefers to situate itself at isolated necks between particles, which may disconnect the channels of open pores. On the contrary, the open pores in the monolithic Al_2O_3 decreased linearly with increasing bulk density. This may be due to the fact that the monolithic Al_2O_3 was sintered at 1 350 °C, which was too low to form a liquid phase from impurities. Moreover, the amount of impurities in monolithic Al_2O_3 is less than that in the Al_2O_3/SiC composite. However, the reason that the open pores disappeared dramatically at the bulk density of about 90% is not clear at present, and further work is required.

3.2 Microstructure

Fig.4 shows the thermally etched microstructures of Al_2O_3/SiC composites before and after HIP treatment. It is evident from Figs.4(a) and (b) that the MgO sintering aid promoted the densification of the composites. For the composite without MgO, a number of closed pores remained though it was sintered at high temperature of 1 800°C. After HIP, however, the Al_2O_3/SiC nanocomposites were completely densified, and the microstructures became indistinguishable, producing similar features and grain sizes regardless of the MgO addition, as shown in Figs.4(c) and (d).

A plot of grain size against density[24, 26] is very useful to understand the effects of an additive, from a macroscopic viewpoint. As shown in Fig.5(a), if an additive promotes only the densification under an identical sintering condition, point *A* will shift horizontally to point *B*. On the other hand, if it only promotes the grain growth (or coarsening), point *A* will be changed vertically to point *C*. The effect of MgO addition on pure Al_2O_3 under an identical sintering condition is clearly shown in Fig.5(a), which is schematically plotted from the reported data[16, 27]. It is evident that a small amount of MgO would enhance the

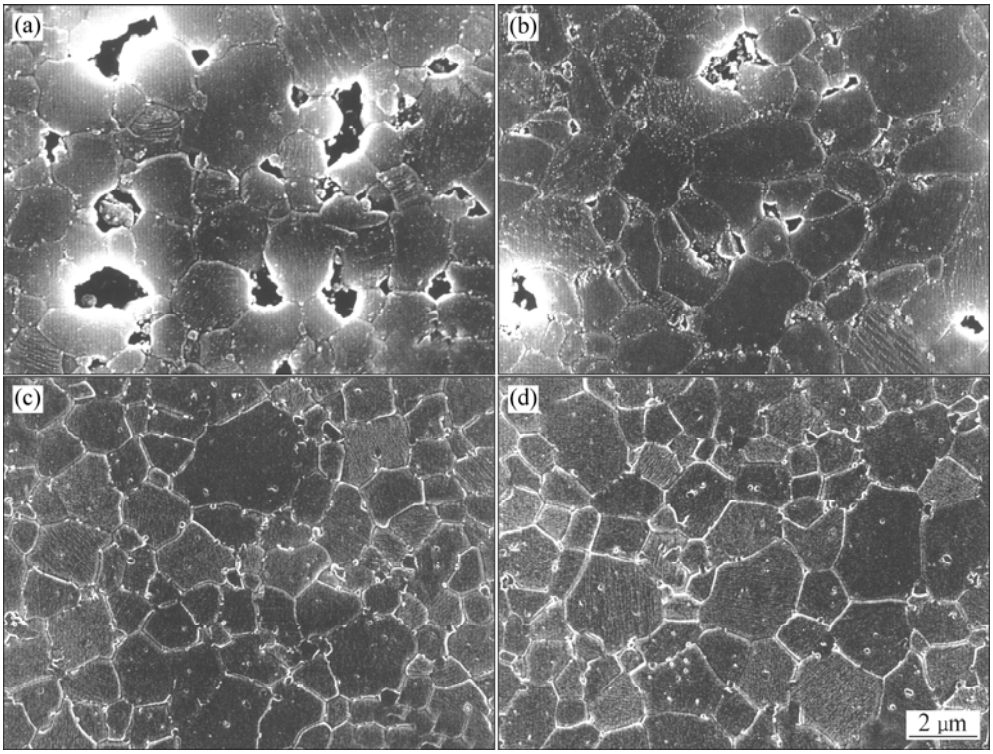

Fig.4 SEM micrographs of thermally etched Al_2O_3/5% SiC nanocomposites sintered at 1 800 °C for 2 h: (a) Without MgO, before HIP; (b) With 0.1% MgO, before HIP; (c) Without MgO, after HIP; (d) With 0.1% MgO, after HIP

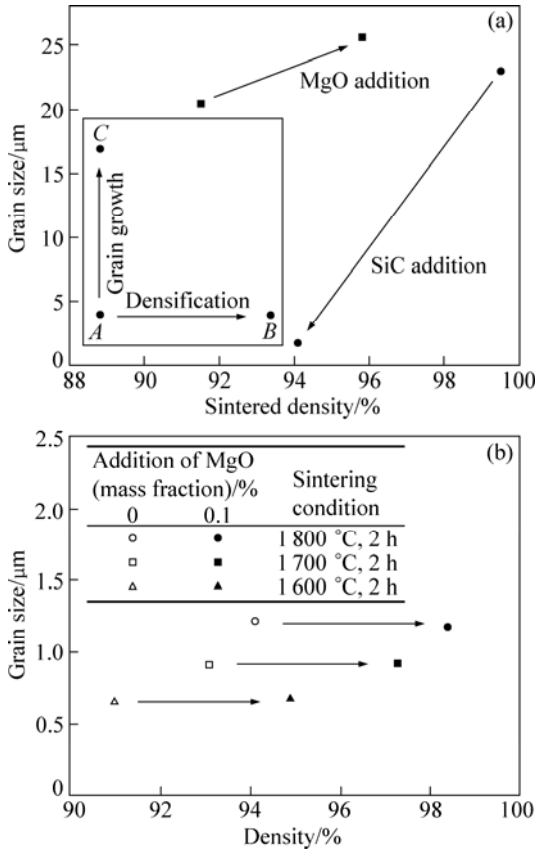

Fig.5 Effect of additive on grain size and density: (a) Proposed role of additive and role of MgO or SiC in pure Al_2O_3 after Harmer[24]; (b) Role of MgO in Al_2O_3/SiC composites

densification and the grain growth of Al_2O_3 during the sintering process, as concluded by BERRY and HARMER[27]. On the contrary, SiC addition to Al_2O_3 retarded the densification and the grain growth of matrix. Thus, it is interesting to observe the effects of MgO in the Al_2O_3/SiC system.

Fig.5(b) shows the effect of MgO addition on the density and grain size of Al_2O_3/SiC composites sintered at different temperatures. As clearly shown, the addition of MgO resulted in promoting only the densification of the composites during the pressureless sintering. However, there were no changes of matrix grain sizes. This suggested that SiC particles effectively inhibited the grain growth of Al_2O_3 matrix in spite of the MgO addition. Hence, it is concluded that the MgO additive can promote the densification of the Al_2O_3/SiC composites, maintaining the inhibition of grain growth by nano-sized SiC particles.

TEM observation of HIP treated Al_2O_3/5%SiC nanocomposites showed that a homogeneous distribution of SiC particles was achieved with particles present both in the Al_2O_3 grains and at the grain boundaries (Fig.6), which was the same as finding in the hot-pressed Al_2O_3/SiC nanocomposites[7−8, 28−30]. Similar features were also obtained by SEM, as shown in Figs.4(c) and (d).

3.3 Fracture strength

Fig.7 shows the variation of the fracture strength as

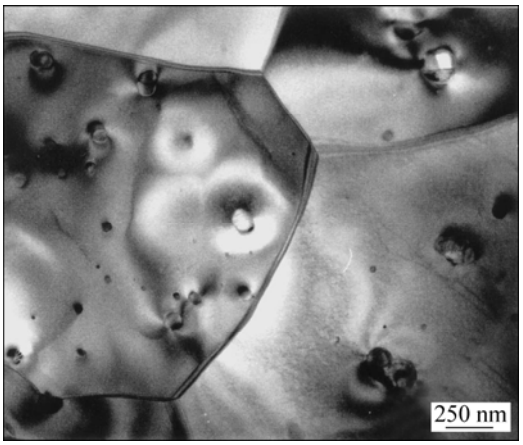

Fig.6 TEM image of Al_2O_3/5%SiC/0.1%MgO nanocomposite fabricated by pressureless sintering at 1 800 °C for 2 h and subsequent HIP treatment at 1 600 °C for 1 h under 150 MPa

a function of the MgO content for Al_2O_3/5%SiC composites before and after HIP treatment. The fracture strength before HIP increased with the MgO content and sintering temperature, owing to the increase of sintered density, as shown in Fig.1. However, the measured strengths are relatively low because of the residual pores, as shown in Figs.4(a) and (b). After HIP treatment, however, high fracture strength of 1 GPa was achieved for the Al_2O_3/5%SiC nanocomposites regardless of the MgO content. (The composite with low strength was not fully densified by HIP, due to the open pores of sintered body). The strength improvement through HIP treatment can be related to the change in fracture mode, as shown in Fig.8. The fracture surface of the sintered body exhibited intergranular and transgranular fracture. On the other hand, the fracture morphology of the HIP treated specimens was identical to that of the hot-pressed Al_2O_3/SiC nanocomposites[9−10, 31], which showed complete transgranular fracture mode.

OHJI et al[32] reported that crack-tip bridging is

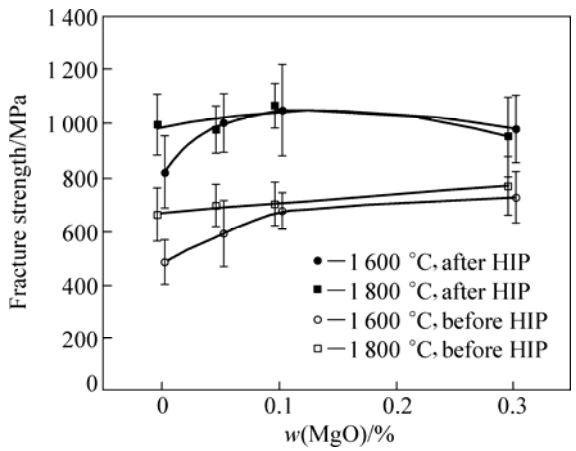

Fig.7 Fracture strength as function of MgO content for Al_2O_3/SiC nanocomposites before and after HIP

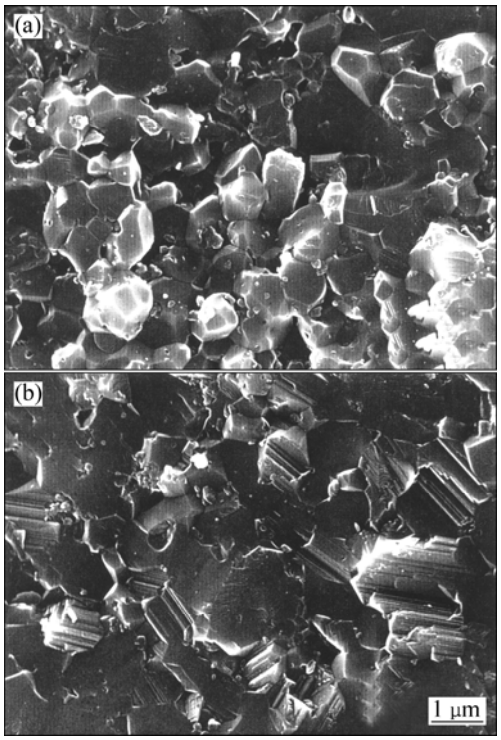

Fig.8 SEM micrographs showing fracture surfaces of Al_2O_3/SiC/0.1% MgO nanocomposite sintered at 1 600 °C for 2 h: (a) Before HIP; (b) After HIP

considered the primary strengthening mechanism of a ceramic nanocomposite. The small, brittle particulate inclusions caused crack-tip bridging at a short distance behind the crack-tip. This mechanism leads to a very steep crack growth resistance curve (*R*-curve), therefore, a high catastrophic fracture strength is attained in the nanocomposites. Crack extension through the nearest SiC particles which was induced by thermal residual tension caused a bridging mechanism to operate effectively, even at a small SiC volume fraction of 5%. From the TEM observation and fracture morphology in the present study, the strengthening mechanism of Al_2O_3/SiC nanocomposites, which is deduced by the pressureless sintering and post HIP process, is believed to be identical with that of hot-pressed nanocomposites.

4 Conclusions

1) The Al_2O_3/5%SiC nanocomposites were successfully fabricated by the pressureless sintering and subsequent HIP process. From the densification behaviors and microstructural observation, MgO additive was effective to improve the densification of Al_2O_3/SiC composites, but had no effect on the grain growth of Al_2O_3 matrix due to the grain growth inhibition by nano-sized SiC particles.

2) The sintered bodies with bulk density higher than

91% were fully densified by HIP treatment. These nanocomposites showed homogeneous distribution of SiC particles, and their fracture morphology was identical with that of the hot-pressed Al_2O_3/SiC nanocomposites showing complete transgranular fracture.

3) Through pressureless sintering and HIP process, the Al_2O_3/5%SiC nanocomposites were able to achieve high fracture strength of 1 GPa, which is the same level with that obtained by hot-pressing. Further, this process can be directly applied to mass production of Al_2O_3/SiC nanocomposites.

References

[1] NIIHARA K, NAKAHIRA A. Strengthening of oxide ceramics by SiC and Si_3N_4 dispersions [C]//Third International Symposium on Ceramic Materials and Components for Engines. Las Vegas: The American Ceramic Society, 1988: 919−926.

[2] NIIHARA K, NAKAHIRA A. SASAKI G. HIRABAYASHI M. Development of strong Al_2O_3/SiC composites [C]//First MRS International Meeting on Advanced Materials. Tokyo: The American Ceramic Society, 1989: 129−134.

[3] NIIHARA K, NAKAHIRA A. Particulate strengthened oxide nanocomposites [C]//7th International Meeting on Modern Ceramics Technologies. Montecatini Terme: The American Ceramic Society, 1990: 637−664.

[4] NIIHARA K. New design concept of structural ceramics: Ceramic nanocomposites [J]. The Centennial Memorial Issue of the Ceramic Society of Japan, 1991, 99(10): 974−982.

[5] NIIHARA K, NAKAHIRA A. Strengthening and toughening mechanisms in nanocomposite [J]. Annales de Chimie, 1991, 16(4): 479−482.

[6] OHJI T, NAKAHIRA A, HIRANO T, NIIHARA K. Tensile creep behavior of alumina/silicon carbide nanocomposites [J]. Journal of the American Ceramic Society, 1994, 77(12): 3259−3262.

[7] OHJI T, HIRANO T, NAKAHIRA A, NIIHARA K. Particle/matrix interface and its role in creep inhibition in alumina/silicon carbide nanocomposites [J]. Journal of the American Ceramic Society, 1994, 79(1): 33−45.

[8] BORSA C E, JIAO S, TODD R I, BROOK R J. Processing and properties of Al_2O_3/SiC nanocomposites [J]. Journal of Microscopy, 1995, 177(3): 305−312.

[9] ZHAO J, STEARNS L C, HARMER M P, CHAN H M, MILLER G A, COOK R. F. Mechanical behavior of alumina-silicon carbide nanocomposites [J]. Journal of the American Ceramic Society, 1993, 76(2): 503−510.

[10] ANYA C C, ROBERTS S G. Pressureless sintering and elastic constants of Al_2O_3-SiC 'nanocomposites' [J]. Journal of the European Ceramic Society, 1997, 17(4): 565−573.

[11] BORSA C E, JONES N M R, BROOK R J, TODD R I. Influence of processing on the microstructural development and flexure strength of Al_2O_3/SiC nanocomposites [J]. Journal of the European Ceramic Society, 1997, 17(6): 865−872.

[12] WALKER C N, BORSA C E, TODD T I, DAVIDGE R W, BROOK R J. Fabrication, characterisation and properties of alumina matrix nanocomposites [C]//Novel Synthesis and Processing of Ceramics, London, 1995: 249−264.

[13] COBLE R L. Sintering crystalline solids. II. Experimental test of diffusion models in powder compacts [J]. Journal of Applied Physics, 1961, 32(793): 793−799.

[14] PEELEN J G J. Sintering and catalysis [M]. New York: Plenum Press, 1975: 443−453.

[15] HARMER M P, ROBERTS E W, BROOK R J. Rapid sintering of pure and doped α-Al_2O_3 [J]. Transactions of the British Ceramic Society, 1979, 78(1): 22−25.

[16] BAE S I, BAIK S. Critical concentration of MgO for the prevention of abnormal grain growth in alumina [J]. Journal of the American Ceramic Society, 1994, 77(10): 2499−2504.

[17] JEONG Y K, NAKAHIRA A, MORGAN P E D, NIIHARA K. Effect of milling conditions on the strength of alumina-silicon carbide nanocomposites [J]. Journal of the American Ceramic Society, 1997, 80(5): 1307−1309.

[18] HÄRDTL K H. Gas isostatic hot pressing without molds [J]. American Ceramic Society Bulletin, 1975, 54(2): 201−207.

[19] TSUKUMA K, SHIMADA M. Hot isostatic pressing of Y_2O_3-partially stabilized zirconia [J]. American Ceramic Society Bulletin, 1985, 64(2): 310−313.

[20] KWON S T, KIM D Y, KANG T K, YOON D Y. Effect of sintering temperature on the densification of Al_2O_3 [J]. Journal of the American Ceramic Society, 1987, 70(4): C69−C70.

[21] SONG H, COBLE R L. Origin and growth kinetics of platelike abnormal grains in liquid-phase-sintered alumina [J]. Journal of the American Ceramic Society, 1990, 73(7): 2077−2085.

[22] LEE C H, KRÖGER F A. Electrical conductivity of polycrystalline Al_2O_3 doped with silicon [J]. Journal of the American Ceramic Society, 1985, 68(2): 92−99.

[23] HANSEN S C, PHILLIPS D S. Grain boundary microstructures in a liquid-phase sintered alumina [J]. Philosophical Magazine A, 1983, 47: 209−234.

[24] HARMER M P. Advances in Ceramics, vol.10 [M]. Columbus: American Ceramic Society, 1984: 679−696.

[25] SHAW T M. Liquid redistribution during liquid-phase sintering [J]. Journal of the American Ceramic Society, 1986, 69(1): 27−34.

[26] YAN M F. Microstructural control in the processing of electronic ceramics [J]. Materials Science and Engineering, 1981, 48(1): 53−72.

[27] BERRY K A, HARMER M P. Effect of MgO solution microstructure development in Al_2O_3 [J]. Journal of the American Ceramic Society, 1986, 69(2): 143−149.

[28] PICIACCHIO A, LEE S H, MESSING G L. Processing and microstructure development in alumina-silicon carbide intragranular particulate composites [J]. Journal of the American Ceramic Society, 1994, 77(8): 2157−2164.

[29] STEARNS L C, ZHAO J, HARMER M P. Processing and microstructure development in Al_2O_3-SiC 'nanocomposites' [J]. Journal of the European Ceramic Society, 1992, 10(6): 473−477.

[30] CARROLL L, STERNITZKE M, DERBY B. Silicon carbide particle size effects in alumina based nanocomposites [J]. Acta Materialia, 1996, 44(11): 4543−4552.

[31] WANG J, PONTON C B, MARQUIS P M. Thermal stability of Al_2O_3-5 % SiC nanocomposite[J]. Journal of Materials Science, 1995, 30(2): 321−333.

[32] OHJI T, JEONG Y K, CHOA Y H, NIIHARA K. Strengthening and toughening mechanisms of ceramic nanocomposites [J]. Journal of the American Ceramic Society, 1998, 81(6): 1453−1460.

(Edited by FANG Jing-hua)